

Effects of Internal Heat Generation and Variable Fluid Properties on Mixed Convection Past a Vertical Heated Plate

P. A. Dinesh¹, N. Nalinakshi² and D. V. Chandrashekhar³

Abstract: Heat and Mass transfer from a vertical heated plate embedded in a sparsely packed porous medium with internal heat generation and variable fluid properties like permeability, porosity and thermal conductivity has been investigated numerically. In particular, the governing highly non-linear coupled partial differential equations are transformed into a system of ordinary differential equations with the help of similarity transformations and solved numerically by using a shooting algorithm based on a Runge-Kutta-Fehlberg scheme and a Newton Raphson method (to obtain velocity, temperature and concentration distributions). The heat and mass transfer characteristics are analyzed and related physical aspects are discussed in detail to interpret the effect of the various significant problem parameters. The results show that the buoyancy ratio number, Prandtl number Pr , Schmidt number Sc and other parameters play an important role. The obtained results are compared with previously published works and they are found to be in very good agreement. The effects of the considered parameters on the local skin friction coefficient (viscous drag), Nusselt number (rate of heat transfer) and Sherwood number (rate of mass transfer) are also discussed.

Keywords: Mixed Convection, porous medium, Internal heat generation, boundary layer.

1 Introduction

Mixed Convection is the flow situation where both free and forced convection effects are of comparable order. Mixed Convection has been over recent years the

¹ Department of Mathematics, M. S. Ramaiah Institute of Technology, MSRIT Post, Bangalore – 560 054, India. E-mail: dinesh_maths@msrit.edu

² Department of Mathematics, Atria Institute of Technology, Bangalore – 560 024, India. E-mail: nalinigcm@yahoo.com

³ Department of Mathematics, Vivekananda Institute of Technology, Bangalore-74, Karnataka, India. E-mail: dvchandru@yahoo.com

subject of much interest due to its relevance to numerous and multivariate applications in the field of air conditioning, heating and refrigeration, in several industrial and technical processes such as electronic devices cooling, nuclear reactors cooled during emergency shut down and heat exchangers placed in a low-velocity environment, geothermal energy extractions, drying of porous solid, thermal insulation and so on. In several physical problems, such as fluids undergoing exothermic and endothermic chemical reaction the study of heat generation is important. Possible heat generation effects may alter the temperature distribution and consequently, the particle deposition rate in nuclear reactors, electric chips and semiconductor wafers. Internal heat generation enhances melting and impedes freezing. This phenomenon occurs in nuclear, geologic, cryogenic and material processing applications. The study of heat generation or absorption effects in moving fluids is important in problem dealing with chemical reactions and those concerned with dissociating fluids such as fluids undergoing exothermic or endothermic chemical reaction.

Several studies have been conducted in this area over a vertical plate with internal heat generation. Vajravelu and Hadjinicolaou (1993) studied the heat transfer characteristics in the laminar boundary layer of a viscous fluid over a stretching sheet with viscous dissipation or frictional heating and internal heat generation. Results of Seddeek (2005) showed that the particle deposition rates were strongly influenced by thermophoresis and buoyancy force, particularly for opposing flow and hot surfaces in his study of the effects of chemical reaction, thermophoresis and variable viscosity on steady hydromagnetic flow with heat and mass transfer over a flat plate in the presence of heat generation absorption. Patil and Kulkarni (2008) studied the effects of chemical reaction on free convective flow of a polar fluid through porous medium in the presence of internal heat generation. Double-diffusive convection radiation interaction on unsteady MHD flow over a vertical moving porous plate with heat generation and solet effects was studied by Mohamed (2009). Ferdows (2011) studied the effect of an exponential form of internal heat generation and variable viscosity in double diffusion problem of MHD from a porous boundary past a continuously moving semi-infinite vertical porous plate. Heat transfer studies in a vertical channel filled with porous medium is analysed by Kamath et al (2013). Mahmoudi et al (2013) made a numerical study of Natural convection in an inclined triangular cavity for different thermal Boundary conditions. Heat transfer and Entropy Analysis for Mixed convection in Discretely Heated Porous square cavity is made by Maougal et al (2013). Moufekkir et al (2012) analysed Numerical study of Double Diffusive Convection in presence of radiating gas in a square cavity.

The review of existing literature relevant to the present work is elaborated in the

following.

Mahrouche et al (2013) studied mixed convection in an opened partitioned Heated cavity and concluded that heat exchange is essentially due to convective cells which by turning bring cooled air from the cold wall to the horizontal faces of the partitions. Numerical and Analytical Analysis of the thermosolutal convection in an Heterogeneous Porous Cavity is studied by Choukairy and Bennacer (2012) and found that heat and mass transfer are doubled while passing from the homogeneous case to the heterogeneous case. Effect of a Porous layer on the flow structure and Heat transfer in a square cavity is studied by Hamimid et al (2012) and concluded that overall heat transfer increases with increasing permeability due to better penetration of the porous layer by the convective flow. The critical conditions for the onset of convection in a doubly diffusive porous layer with internal heat generation were documented by Selimos and Poulikakos (1985). Convective instability study by considering the combined effects of internal heat generation and through flow has been made by Khalili and Shivakumara (1998) who have modelled a solar pond by allowing q''' varying exponentially with depth, including the effect of vertical through flow. The heat generation effects on steady combined free-forced convection and mass transfer flow past a semi-infinite vertical porous flat plate embedded in a porous medium was studied by Alam et al (2006) and concluded that volumetric heat generation term exerts a strong influence on the heat transfer and also on the fluid flow. They also observed that suction stabilizes the boundary layer growth and sucking decelerated fluid particles through the porous wall reduce the growth of the fluid boundary layer as well as thermal and concentration boundary layers.

The effect of heat generation, viscous dissipation on free convection heat and mass transfer from a vertical wall in a doubly stratified, fluid saturated, Darcy porous medium was studied by Govardhan et al (2012). Vajravelu (1980) studied the effects of variable properties and internal heat generation on natural convection at a heated vertical plate in air and observed that wall heat transfer coefficient in the variable fluid property case is about 30% higher than in the constant fluid property case. The presence of heat sources delays attainment of the steady-state condition. Mixed convection from a convectively heated vertical plate to a fluid with internal heat generation approach is made by Makinde and Aziz (2011), by considering the cold fluid flowing over the right face of the plate containing a heat generation that decays exponentially with a dimensionless distance from the wall. In the development of a metal waste from spent nuclear fuel, phase change processes and thermal combustion processes, convection with internal heat generation plays an important role in the overall heat transfer process. Crepeau and Clarksean (1997) considered the classical problem of natural convection from an isothermal vertical plate and

added a heat generation term in the energy equation and found that for a true similarity solution to exist, the internal heat generation must decay exponentially with the classical similarity variable. Olanrewaju et al (2012) investigated the internal heat generation effect on thermal boundary layer with a convective surface boundary condition over a flat plate and concluded that because of strong internal heat generation the plate surface temperatures exceed the temperature of the fluid on the lower surface of the plate and the direction of heat flow is reversed. Ali Chamkha (2007) studied heat and mass transfer for a non-Newtonian fluid flow along a surface embedded in a porous medium with uniform wall heat and mass fluxes and heat generation or absorption and found that increasing the heat generation or absorption parameter decreases the local Nusselt number and increasing the Lewis number produced increases in the local Sherwood number.

In some industrial applications, such as fixed-bed catalytic reactors, packed bed heat exchangers and drying, the value of the porosity is maximum at the wall and minimum away from the wall, so the porosity of the porous medium should be taken as non-uniform.

Porosity measurements by Shwartz and Smith (1953) and Benenati and Brosilow (1962) show that porosity is not constant but varies from the wall to the interior of the porous medium due to which permeability also varies. Chandrasekhara et al (1985) has incorporated the variable permeability to study the flow past and through a porous medium and have shown that the variation of porosity and permeability has greater influence on velocity distribution and on heat transfer. Nevertheless, the inertia effects become important in a sparsely packed porous medium and hence their effect on mixed convection problems needs to be investigated. Mohammedin and El-shaer (2004) studied mixed convective flow past a semi-infinite vertical plate embedded in a porous medium incorporating the variable permeability in Darcy's model. Recently, Pal and Shivakumar (2006) analyzed mixed convection heat transfer from a vertical heated plate embedded in a Newtonian fluid sparsely packed porous medium by considering the variation of permeability, porosity and thermal conductivity. Dulal Pal (2010) studied magnetohydrodynamic non-Darcy mixed convection heat transfer from a vertical heated plate embedded in a porous medium with variable porosity, by taking the viscous dissipation term in the energy equation. Nalinakshi et al (2013) analyzed numerically Double Diffusive mixed convection with variable fluid properties.

Further studies along these lines, for different geometries will help to find the right combination that promotes heat and mass transfer and thus better cooling. In the present paper, in particular we study systematically and numerically the mixed convection heat and mass transfer for a Newtonian fluid flow past a semi infinite vertical heated plate embedded in a sparsely packed porous medium incorporating

the variable porosity, permeability and thermal conductivity in the presence of Internal Heat Generation (IHG). To achieve this objective our plan of work is, in the analysis highly coupled non-linear partial differential equations governing the physical system are first reduced by a similarity transformations to the ordinary differential equations and then the resultant boundary value problem is converted into the system of seven simultaneous equations of first-order for seven unknowns. These equations are solved numerically by shooting technique by Runge-Kutta-Fehlberg Methods to obtain velocity, temperature and concentration profiles for various physical parameters.

2 Mathematical Formulation

Two-dimensional, laminar, steady- state boundary layer flows of an incompressible fluid past a semi-infinite vertical heated plate embedded in a sparsely packed Newtonian fluid saturated porous medium of variable porosity, permeability and thermal conductivity with IHG is considered. The x-coordinate is measured along the plate from its leading edge, and y-coordinate normal to it. Let U_0 be the velocity of the fluid in the upward direction and the gravitational field, g , is acting in the downward direction. The plate is maintained at a uniform temperature T_w and at uniform concentration C_w which is always greater than the free stream values existing far from the plate (*i.e.*, $T_w > T_\infty$ and $C_w > C_\infty$).

Considering the theory of boundary layer effect for sparsely packed porous medium with high porosity ε (but less than unity), the general vectorial equations for the conservation of mass, momentum, energy and species concentration for steady, viscous, incompressible, Newtonian fluid flow can be written as:

Continuity equation:

$$\nabla \cdot \vec{q} = 0 \quad (1)$$

Momentum equation:

$$\rho_o (\vec{q} \cdot \nabla) \vec{q} = -\nabla \rho + \rho \vec{g} + \bar{\mu} \nabla^2 \vec{q} - \frac{\mu \varepsilon}{k} \vec{q}, \quad (2)$$

Energy equation:

$$(\rho_o C_p) (\vec{q} \cdot \nabla) T = \nabla \cdot (\kappa \nabla T) + \Phi + q''', \quad (3)$$

Concentration equation:

$$(\vec{q} \cdot \nabla) C = \kappa_c \cdot \nabla^2 C + \Phi, \quad (4)$$

where $\vec{q} = (u, v)$, u and v are the velocity components along the x and y directions, respectively. ρ is the density of the fluid, \vec{g} is the acceleration due to gravity, p is the pressure, T is the temperature of the fluid, C is the concentration of the fluid, $\bar{\mu}$ is the effective viscosity of the fluid, μ is the fluid viscosity, C_p is the specific heat at constant pressure, κ is the variable thermal conductivity, κ_c is the solutal diffusivity, β_T is the coefficient of volume expansion, β_C is the volumetric coefficient of expansion with species concentration, q''' is the exponential form of (IHG) and ϕ is the viscous dissipation term.

With the assumptions: (a) The Bousinesque approximation is valid i.e., density is constant everywhere in the momentum equation except in the buoyancy force. (b) Permeability, porosity, thermal resistance solutal diffusivity are functions of the vertical coordinate y (c) Local thermal equilibrium exists between fluid and solid phase.

The governing basic equations (1) – (4) for steady two-dimensional flow can be written in the form:

Continuity equation:

$$u \frac{\partial u}{\partial x} + v \frac{\partial u}{\partial y} = 0, \tag{5}$$

Momentum equation:

$$u \frac{\partial u}{\partial x} + v \frac{\partial u}{\partial y} = -\frac{1}{\rho_o} \frac{\partial p}{\partial x} + g\beta_T (T - T_\infty) - g\beta_C (C - C_\infty) + \frac{\bar{\mu}}{\rho_o} \frac{\partial^2 u}{\partial y^2} - \frac{\mu}{\rho_o} \frac{\varepsilon(y)}{k(y)} u, \tag{6}$$

Energy equation:

$$u \frac{\partial T}{\partial x} + v \frac{\partial T}{\partial y} = \frac{\partial}{\partial y} \left(\alpha(y) \frac{\partial T}{\partial y} \right) + q''' + \frac{\bar{\mu}}{\rho C_p} \left(\frac{\partial u}{\partial y} \right)^2, \tag{7}$$

Concentration equation:

$$u \frac{\partial C}{\partial x} + v \frac{\partial C}{\partial y} = \gamma_m \frac{\partial^2 C}{\partial y^2}, \tag{8}$$

where, $\Phi = \frac{\bar{\mu}}{\rho_o C_p} \left(\frac{\partial u}{\partial y} \right)^2$, T_∞ is the ambient temperature, C_∞ is the ambient concentration, $k(y)$ the variable permeability of the porous medium is, $\varepsilon(y)$ is the variable porosity of the saturated porous medium, $\alpha(y)$ is the variable effective thermal diffusivity of the medium and γ_m is the effective solutal diffusivity of the medium. For simplicity we consider $\rho = \rho_o$.

To determine the flow field the above governing equations need to be solved subject to the boundary conditions. The different types of rigid surfaces boundary conditions have been stated to describe flow characteristics at the boundary, near the plate and far away from the plate embedded in a sparsely packed porous medium.

The following are the boundary conditions on velocity, temperature and concentration fields:

$$u = 0, \quad v = 0, \quad T = T_w, \quad C = C_w \quad \text{at} \quad y = 0, \tag{9}$$

$$u = U_o, \quad v = 0, \quad T = T_\infty, \quad C = C_\infty \quad \text{as} \quad y \rightarrow \infty \tag{10}$$

Since the flow field is uniform at a sufficiently large distance from the porous surface, the free stream U_o where U_o is the free stream velocity. The expression for free stream velocity is obtained from Equation (2) and is given by,

$$\frac{1}{\rho} \frac{\partial p}{\partial x} = -\frac{\mu \varepsilon(y)}{\rho k(y)} U_o. \tag{11}$$

Eliminating $\frac{\partial p}{\partial x}$ in equation (6) by using equation (11), we finally obtain the momentum equation as:

$$u \frac{\partial u}{\partial x} + v \frac{\partial u}{\partial y} = \vec{g} \beta_T (T - T_\infty) - \vec{g} \beta_C (C - C_\infty) + \frac{\bar{\mu}}{\rho} \frac{\partial^2 u}{\partial y^2} + \frac{\mu \varepsilon(y)}{\rho k(y)} (U_o - u). \tag{12}$$

Equations (5), (7), (8) & (12) are highly nonlinear partial differential equations, in order to solve them the following dimensionless variables f , θ , ϕ , and q''' and as well as the similarity variable η are introduced (see Hady et al [175], Mohammadein and El-shaer [33]):

$$\eta = \left(\frac{y}{x}\right) \left(\frac{U_o x}{\nu}\right)^{1/2}, \quad \Psi = \sqrt{\nu U_o x} f(\eta), \quad \theta = \frac{T - T_\infty}{T_w - T_\infty}, \tag{13}$$

$$\phi = \frac{C - C_\infty}{C_w - C_\infty}, \quad q''' = \frac{U_o (T_w - T_\infty)}{2x} e^{-\eta},$$

where ν is the kinematic viscosity of the fluid, $\psi = \psi(x, y)$ is the stream function defined by $u = \frac{\partial \psi}{\partial y}$, $v = -\frac{\partial \psi}{\partial x}$ is such that the continuity equation (5.5) is satisfied automatically and the velocity components are given by

$$u = U_o f'(\eta), \quad v = -\frac{1}{2} \sqrt{\frac{\nu U_o}{x}} (f(\eta) - \eta f'(\eta)). \tag{14}$$

The variable permeability $k(\eta)$, the variable porosity $\varepsilon(\eta)$ and the variable effective thermal diffusivity $\alpha(\eta)$ are given by, following the study made by Chandrasekhara and Namboodiri [31]

$$k(\eta) = k_o (1 + d e^{-\eta}), \tag{15}$$

$$\varepsilon(\eta) = \varepsilon_o (1 + d^* e^{-\eta}), \tag{16}$$

$$\alpha(\eta) = \alpha_o [\varepsilon_o (1 + d^* e^{-\eta}) + \sigma^* \{1 - \varepsilon_o (1 + d^* e^{-\eta})\}], \tag{17}$$

where k_o , ε_o , α_o are the permeability, porosity and diffusivity at the edge of the boundary layer respectively, σ^* is the ratio of the thermal conductivity of solid to the conductivity of the fluid, d and d^* are treated as fixed constants for variable permeability (VP) and $d = d^* = 0$ for uniform permeability (UP).

Equations (7), (8) & (12) are transformed into ordinary differential equations by substituting the dimensionless variables introduced in equations (13) to (17), the simplified local similarity equations are

$$f''' = -\frac{1}{2} f f'' - \frac{Gr}{Re^2} (\theta - N\phi) - \frac{\alpha^*}{\sigma Re} \left(\frac{1 + d^* e^{-\eta}}{1 + d e^{-\eta}} \right) (1 - f'), \tag{18}$$

$$\theta'' = \frac{-\frac{1}{2} Pr f \theta' - Pr E f'^2 - \frac{1}{2} Pr e^{-\eta} - \varepsilon_o d^* e^{-\eta} (\sigma^* - 1) \theta'}{\varepsilon_o + \sigma^* (1 - \varepsilon_o) + \varepsilon_o d^* e^{-\eta} (1 - \sigma^*)}, \tag{19}$$

$$\phi'' = -\frac{1}{2} Sc f \phi', \tag{20}$$

where, $Pr = \bar{\mu} / \rho \alpha_o$ is the Prandtl number, $Sc = \bar{\mu} / \rho \gamma_o$ is the Schmidt number, N , β^* , $\alpha^* / \sigma Re$, Gr / Re^2 is the ratio of viscosities, $N = \frac{\beta_C (C_w - C_\infty)}{\beta_T (T_w - T_\infty)}$ is the Buoyancy ratio, $E = U_o^2 / C_p (T_w - T_\infty)$ is the Eckert number, $\sigma = k_o / x^2 \varepsilon_o$ is the local permeability parameter, $Re = U_o x / \nu$ is the local Reynolds number and $Gr_T = g \beta_T (T_w - T_\infty) x^3 / \nu^2$ is the thermal Grashof number, $Gr_C = g \beta_C (C_w - C_\infty) x^3 / \nu^2$ is the solutal Grashof number. $\frac{Gr}{Re^2}$ is the mixed convection parameter called as Richardson number and $Gr_T = Gr_C$.

The transformed boundary conditions are:

$$f = 0, \quad f' = 0, \quad \theta = 1, \quad \phi = 1 \quad \text{at} \quad \eta = 0, \tag{21}$$

$$f' = 1, \quad \theta = 0, \quad \phi = 0 \quad \text{as} \quad \eta \rightarrow \infty. \tag{22}$$

Once the velocity, temperature and concentration distributions are known, for many practical applications, it is important to find an expression for the skin friction, the rate of heat transfer and the rate of mass transfer. The Nusselt number is defined as the ratio of the vertical heat flux to the conductive vertical heat flux. In the steady state the vertical heat flux is independent of the vertical coordinate. Hence, they can be calculated respectively by using (as discussed in chapter 4)

$$\tau = -f''(0) / \sqrt{Re}, \quad Nu = -\sqrt{Re} \theta'(0) \quad \text{and} \quad Sh = -\sqrt{Re} \phi'(0), \tag{23}$$

where τ is the skin friction, Nu is the Nusselt number and Sh is the Sherwood number.

3 Method of Solution

The boundary value problem arising due to vertical heated plate are highly coupled nonlinear ordinary differential equations (ODE's) which are difficult to solve analytically, we employ one of the numerical technique called the shooting method to solve the obtained coupled ODE's. By this method, first we try to transform the coupled ODE's (18) – (20) into the system of simultaneous first order ODE's and converting Boundary Value Problem (BVP) to Initial Value Problem (IVP) by choosing a suitable guess value at the initial point. The obtained first order ODE's with the corresponding initial condition are solved by employing Runge-Kutta-Fehlberg Integration method. The method is illustrated as given below:

1. Decision on ∞ .
2. Converting BVP to IVP by choosing suitable initial condition for f , θ , ϕ .
3. $f''(0)$, $\theta'(0)$ and $\phi'(0)$ required for the solution of initial value problem are chosen by the classical, explicit Runge-Kutta Fehlberg method of fourth order.

The decision on an appropriate ' ∞ ' for the problem depends on the proper parameter values chosen. In view of this, for each parameter combination, the appropriate value of ' ∞ ' has to be decided. The algorithm for the shooting method with Runge-Kutta fourth order approximating is used.

Initially, we chose guess values as $f''(0) = P$, $\theta'(0) = Q$ and $\phi'(0) = R$. The process of obtaining P , Q and R accurately involves iteration process and can be calculated, repeating the same calculation we get another improved value, but these chosen guess values are not the most accurate values and hence there is a need to redefine. The better guess can be obtained by using the Newton-Raphson method. We solve the equations (18)-(20) with initial conditions

$$\begin{aligned} f(0) = 0, \quad f'(0) = 0, \quad f''(0) = P, \quad \theta(0) = 1, \\ \theta'(0) = Q, \phi(0) = 1, \quad \phi'(0) = R. \end{aligned} \tag{24}$$

Due to crude choice of $f''(0)$, $\theta'(0)$ and $\phi'(0)$, the solution at ' ∞ ' does not match with those given in the problem using the classical explicit Runge-Kutta method of fourth order. Thus, the coupled nonlinear boundary value problem (BVP) of third-order in $f(\eta)$ and second-order in $\theta(\eta)$ and $\phi(\eta)$ has been reduced to a system of seven simultaneous equations of first-order for seven unknowns as follows (see

Vajravelu [176]):

$$\begin{aligned}
 f &= f_1, & \frac{df_1}{d\eta} &= f_2, & \frac{df_2}{d\eta} &= f_3, \\
 \frac{df_3}{d\eta} &= -\frac{1}{2}f_1f_3 - \frac{Gr}{Re^2}(f_4 - Nf_6) - \frac{\alpha^*(1 + d^*e^{-\eta})}{\sigma Re(1 + de^{-\eta})}(1 - f_2), \\
 \theta &= f_4, & \frac{df_4}{d\eta} &= f_5, \\
 \frac{df_5}{d\eta} &= -\frac{(1/2)Pr f_1f_5 + Pr E f_3^2 + (1/2)Pr e^{-\eta} + \epsilon_0 d^* e^{-\eta} (\sigma^* - 1) f_5}{\epsilon_0 + \sigma^*(1 - \epsilon_0) + \epsilon_0 d^* e^{-\mu}(1 - \sigma^*)}, \\
 \phi &= f_6, & \frac{df_6}{d\eta} &= f_7, & \frac{df_7}{d\eta} &= -\frac{1}{2}Sc f_1 f_7.
 \end{aligned} \tag{25}$$

where $f_1 = f, f_2 = f', f_3 = f'', f_4 = \theta, f_5 = \theta', f_6 = \phi, f_7 = \phi'$ and a prime denotes differentiation with respect to η . The boundary conditions (21) and (22) will now take the form.

$$\begin{aligned}
 f_1(0) &= 0, & f_2(0) &= 0, & f_3(0) &= P, & f_4(0) &= 1, \\
 f_5(0) &= Q, & f_6(0) &= 1, & f_7(0) &= R,
 \end{aligned} \tag{26}$$

$$f_2(\infty) = 1, \quad f_4(\infty) = 0, \quad f_6(\infty) = 0. \tag{27}$$

To solve the system of first-order differential equations along with boundary conditions, we need seven initial conditions, but we have only two initial conditions on $f(\eta)$, one initial condition on $\theta(\eta)$ and one initial condition on $\phi(\eta)$. The third condition of f (i.e. $f''(0)$), second condition on θ (i.e. $\theta'(0)$) and second condition on ϕ (i.e. $\phi'(0)$) are not prescribed, which are determined by employing numerical shooting method and using the two ending boundary condition given in equation (27). The selection of an appropriate finite value of η_∞ is to be made. A good guess of the initial condition in the shooting technique is to be made on which the convergence depends. The accuracy of the assumed initial conditions is checked by comparing the calculated values of the dependent variable at the terminal point with its given value at that point. If any difference exists, improved values of the assumed initial conditions must be obtained and the process is repeated. The iterative process is terminated when the difference between two successive values reached 10^{-6} , then the solution is said to have converged results. The slight deviation in the values may be due to the use of Runge-Kutta-Fehlberg method which has fifth order accuracy whereas; Mohammadein and El-Shaer (2004) have used fourth-order Runge-Kutta method which has only fourth order accuracy who has analysed the influence of variable permeability with heat transfer in the absence of IHG. Thus the present results are more accurate compared to their results.

4 Results and Discussion

The flow of steady, laminar, incompressible viscous fluid in a vertical heated plate embedded in a saturated porous medium has been investigated in presence of internal heat generation in the energy equation. The Brinkman extended Darcy equation is used along with the continuity equation, energy and species concentration equation to illustrate the flow behavior in sparsely packed porous medium. The exponential form of internal heat generation is considered. The partial differential equations are converted into ordinary differential equation using the similarity solution method. The system of first-order differential equations (18)-(20) are solved numerically using shooting technique with Runge-Kutta-Fehlberg method. In order to know the accuracy of the method used, computed values of $f''(0)$, $\theta'(0)$ and $\phi'(0)$ were obtained for buoyancy ratio $N = 0$ and compared with those obtained by Mohammadein and El-Shaer (2004) with only the heat transfer, for the variable permeability case and good agreement has been obtained with their results. The values are tabulated in the Table 1, 2 for $\varepsilon_o = 0.4$, $Ec = 0.1$, $Pr=0.71$, $Sc=0.22$ with selected values of Gr/Re^2 , σ^* , N and $\alpha^*/\sigma Re$ for both uniform permeability (UP) (*i.e.*, $d = d^* = 0.0$) and variable permeability (VP) (*i.e.*, $d = d^* \neq 0$) cases. For the purpose of numerical integration we have assumed $d = 3.0$ and $d^* = 1.5$ (chandrashekhara et al (1985)). The slight deviation in the values may be due to the use of Runge-Kutta-Fehlberg method which has fifth order accuracy. Table 3, 4 shows the values of local Nusselt number and local Sherwood number ($-\theta'(0)$ and $-\phi'(0)$) for $Ec = 0.1$, $\alpha^*/\sigma Re = 0.1$, $N=1.0$, for both Uniform Permeability (UP) and Variable Permeability (VP) cases for different values of Pr and Sc respectively.

As a result of the numerical calculations, the dimensionless velocity, temperature and concentration distributions for the flow under consideration are obtained and their behaviour have been discussed for various non-dimensional parameters.

The velocity distributions for various values of buoyancy ratio N have been depicted in Fig.1. It is observed that increase in the value of buoyancy ratio N there is a slight increase in the velocity profile and the boundary layer also varies slightly. The temperature distributions are shown for various values of buoyancy ratio N in Fig. 2, it is observed that increase in value of buoyancy ratio N there is a decrease in the temperature profile. When the buoyancy ratio the boundary layer smoothly deviates very slowly, when the buoyancy ratio starts with $N = 1$, there is a decrease in the temperature boundary layer very faster and further increase continues with the same behaviour. This shows that heat transfer is faster as we increase buoyancy ratio parameter due to the presence of the internal heat generation term which is an exponential term. The concentration profiles are shown for various values of buoyancy ratio N in Fig. 3, it is observed that increase in value of buoyancy ratio N there is a decrease in the concentration profile similar to the temperature profile,

whereas the rapid decrease starts when $N = 5$.

Table 1: Results for $f''(0)$, $-\theta'(0)$ and $\phi'(0)$ for $Pr=0.71$, $Sc=0.22$, $Ec=0.1$ and $\epsilon_0=0.4$ for Uniform Permeability (UP) cases with Internal Heat Generation.

N	σ^*	Gr/Re^2	$\alpha^*/\sigma Re$	Uniform Permeability (UP)			
				$f''(0)$	$-\theta'(0)$	$-\phi'(0)$	
0	2	0.0	0.0	0.354671	0.246540	0.248640	
			0.1	0.446543	0.293567	0.298751	
			0.5	0.771564	0.382654	0.388657	
		0.2	0.0	0.786550	0.426550	0.429850	
			0.1	0.856509	0.567800	0.574200	
			0.5	0.998750	0.587650	0.593450	
		2.0	0.0	1.345650	0.790045	0.796650	
			0.1	1.396500	0.889950	0.905500	
			0.5	1.654550	0.987540	0.993540	
	4	0.2	0.1	0.946789	0.601546	0.608756	
	1	2	0.0	0.0	0.400350	0.294503	0.299900
				0.1	0.465650	0.324565	0.329550
0.5				0.778550	0.425500	0.429650	
0.2			0.0	0.790054	0.543500	0.549500	
			0.1	0.824535	0.567430	0.572340	
			0.5	0.984565	0.651789	0.641456	
2.0			0.0	1.437868	0.658976	0.659880	
			0.1	1.521784	0.689450	0.694550	
			0.5	1.734256	0.789450	0.795550	
4		0.2	0.1	0.996754	0.589341	0.561132	
5		2	0.2	0.1	1.036789	0.675431	0.650034
				0.5	1.456782	0.681432	0.670134
10	2	0.2	0.1	1.558978	0.743451	0.731342	
			0.5	1.778956	0.781322	0.779432	

Table 2: Results for $f''(0)$, $-\theta'(0)$ and $\phi'(0)$ for $Pr=0.71$, $Sc=0.22$, $Ec=0.1$ and $\epsilon_0=0.4$ for Variable Permeability (VP) with Internal Heat Generation.

N	σ^*	Gr/Re^2	$\alpha^*/\sigma Re$	Variable Permeability (VP)			
				$f''(0)$	$-\theta'(0)$	$-\phi'(0)$	
0	2	0.0	0.0	0.353800	0.282750	0.280750	
			0.1	0.435670	0.325750	0.328590	
			0.5	0.675800	0.400580	0.400780	
		0.2	0.0	0.425600	0.400990	0.401205	
			0.1	0.534500	0.541456	0.545672	
			0.5	0.778500	0.561578	0.567652	
		2.0	0.0	1.345670	0.781453	0.794323	
			0.1	1.378900	0.881132	0.901256	
			0.5	2.004500	0.980023	0.988976	
	4	0.2	0.1	0.552345	0.584573	0.571562	
	1	2	0.0	0.0	0.356590	0.287500	0.286500
				0.1	0.426789	0.300670	0.300470
0.5				0.777850	0.456700	0.456100	
0.			0.0	0.784565	0.489650	0.486950	
			0.1	0.813453	0.498540	0.497530	
			0.5	0.945675	0.685933	0.683915	
2.0			0.0	1.456873	0.756800	0.755800	
			0.1	1.531562	0.785933	0.782134	
			0.5	1.739874	0.876540	0.874786	
4		0.2	0.1	0.912354	0.523456	0.552004	
5		2	0.2	0.1	0.995432	0.657875	0.651053
				0.5	1.405673	0.677892	0.670001
10	2	0.2	0.1	1.554322	0.734561	0.729324	
			0.5	1.740345	0.775641	0.767891	

Table 3: Values of local Nusselt number with fixed $Ec = 0.1$, $\epsilon_0=0.4$, $\alpha^*/\sigma Re=0.1$ and $N=1.0$, for Uniform Permeability (UP) and Variable Permeability (VP) cases for different values of Pr.

Gr/Re^2	Pr = 0.71		Pr = 3.0		Pr = 7.0	
	$-\theta'(0)$		$-\theta'(0)$		$-\theta'(0)$	
	UP	VP	UP	VP	UP	VP
0.0	0.42768	0.43578	0.45987	0.49567	0.54655	0.55675
0.2	0.43568	0.45168	0.48679	0.52343	0.56123	0.58345
2.0	0.44659	0.49687	0.53673	0.57145	0.58145	0.63564

Table 4: Values of local Sherwood number with fixed $Ec = 0.1$, $\epsilon_o=0.4$, $\alpha^*/\sigma Re=0.1$ and $N=1.0$, for Uniform Permeability (UP) and Variable Permeability (VP) cases for different values of Sc .

Gr/Re^2	$Sc = 0.22$		$Sc = 0.44$		$Sc = 0.60$	
	$-\phi'(0)$		$-\phi'(0)$		$-\phi'(0)$	
	UP	VP	UP	VP	UP	VP
0.0	0.43168	0.44578	0.47987	0.51567	0.55655	0.57675
0.2	0.43568	0.45168	0.48679	0.52343	0.56123	0.58345
2.0	0.44659	0.49687	0.53678	0.57145	0.58145	0.63564

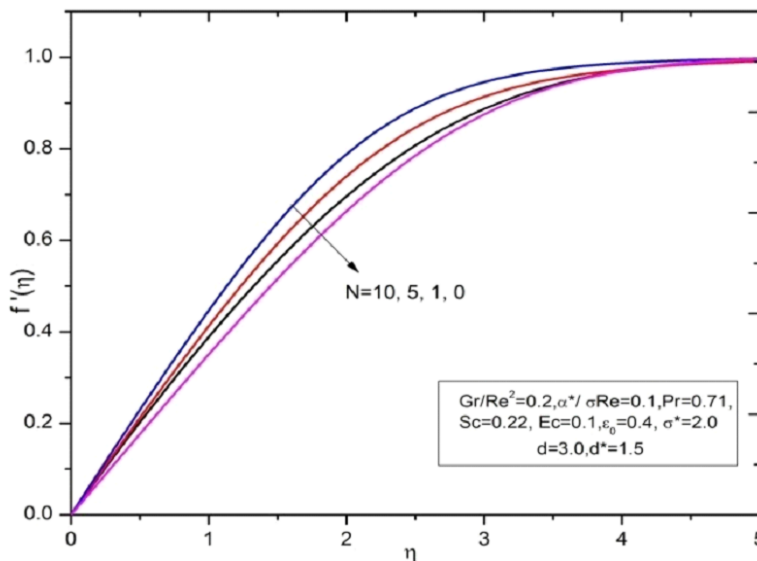


Figure 1: Velocity distributions for various values of buoyancy ratio N for VP case.

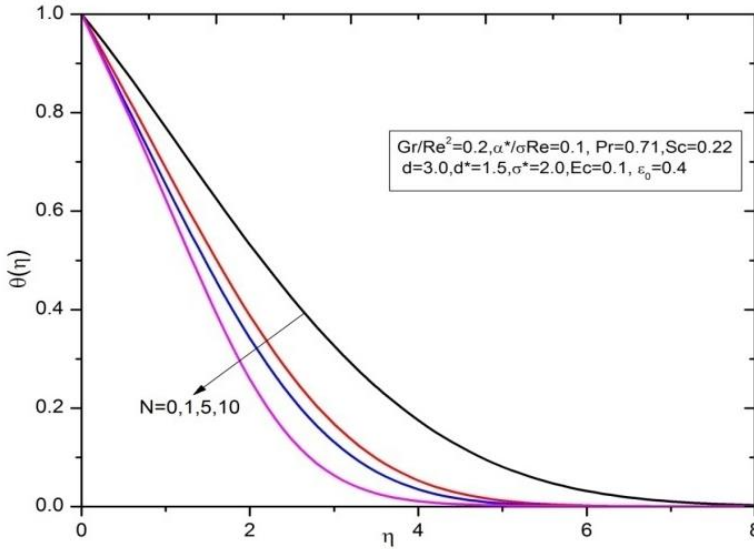


Figure 2: Temperature distributions for various values of buoyancy ratio N for VP case.

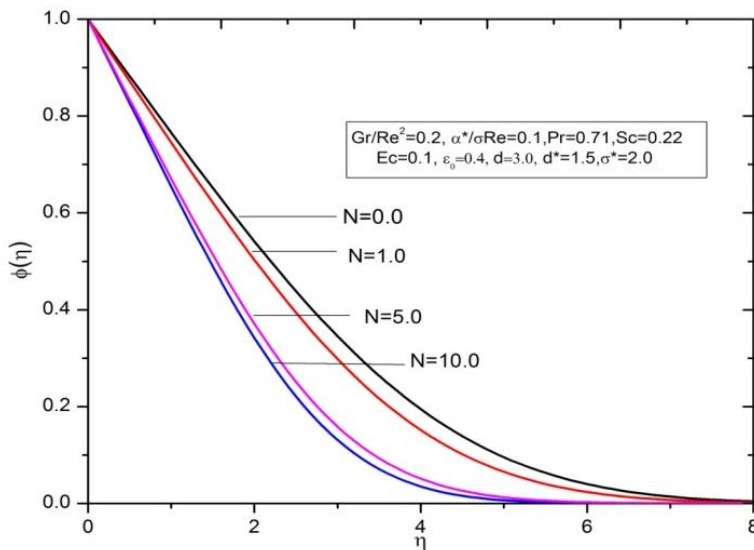


Figure 3: Concentration distribution for various values of buoyancy ratio N for VP case.

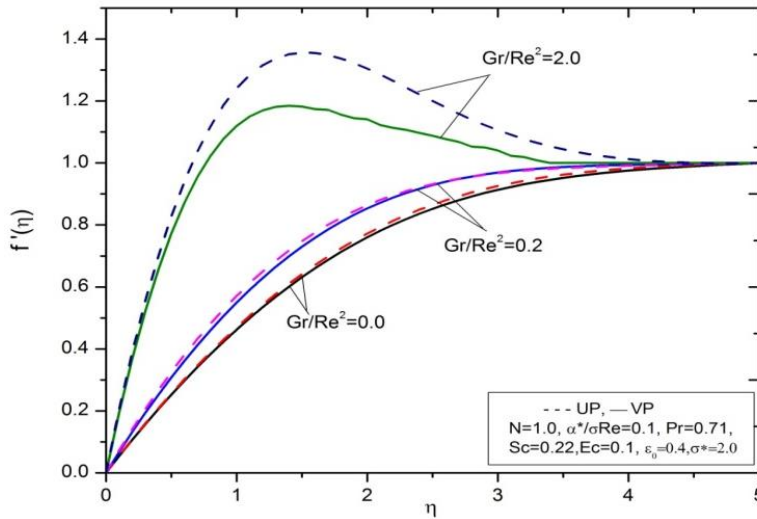


Figure 4: Velocity distributions for various values of Gr/Re^2 for both UP and VP cases.

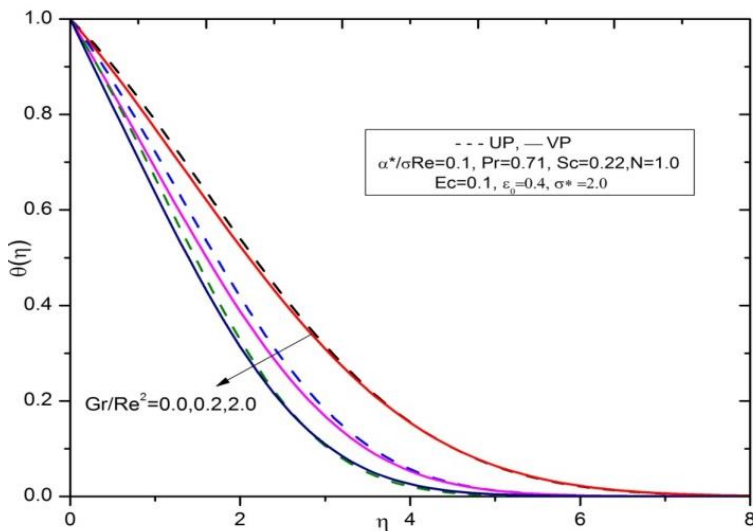


Figure 5: Temperature distributions for various values of Gr/Re^2 for both UP and VP cases.

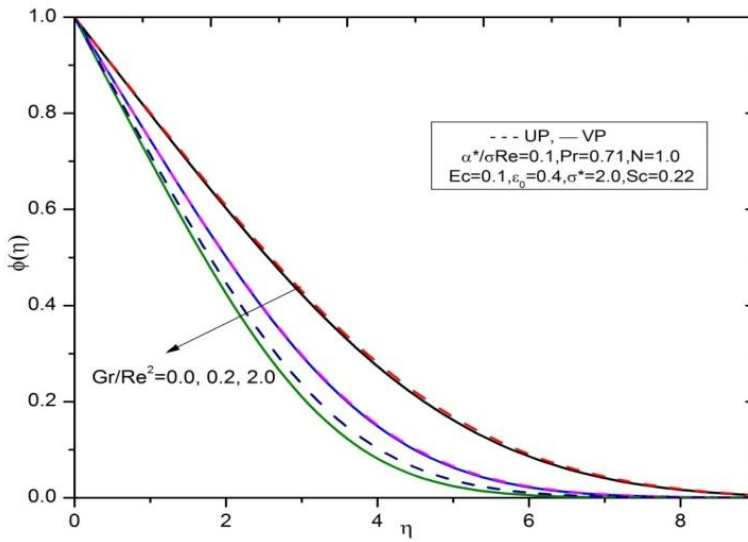


Figure 6: Concentration profiles for different values of Gr/Re^2 for both UP and VP cases.

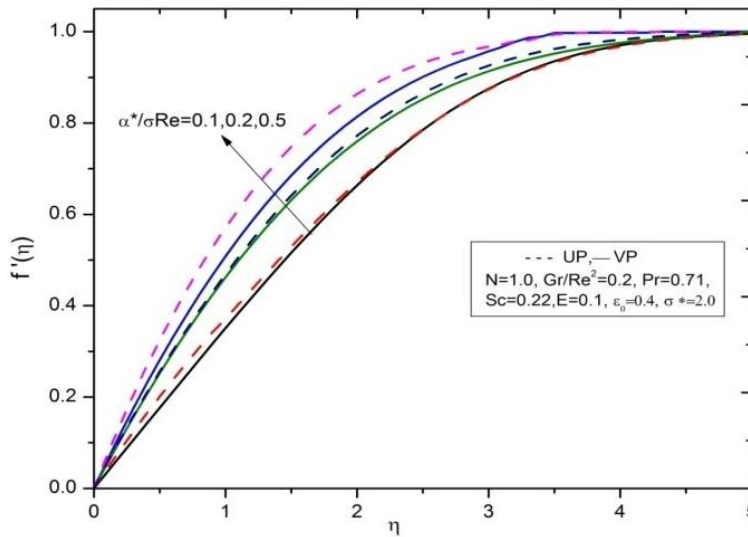


Figure 7: Velocity profiles for various values of $\alpha^*/\sigma Re$ for UP and VP cases.

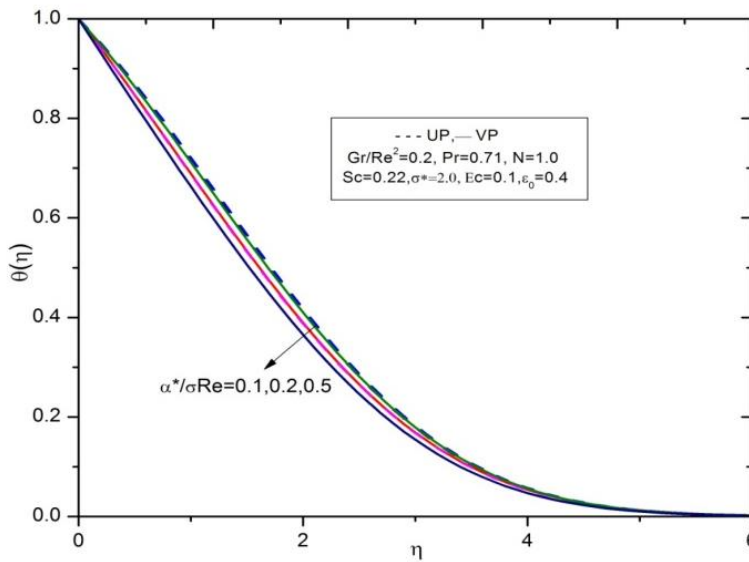


Figure 8: Temperature profiles for various values of $\alpha^*/\sigma Re$ for UP and VP cases.

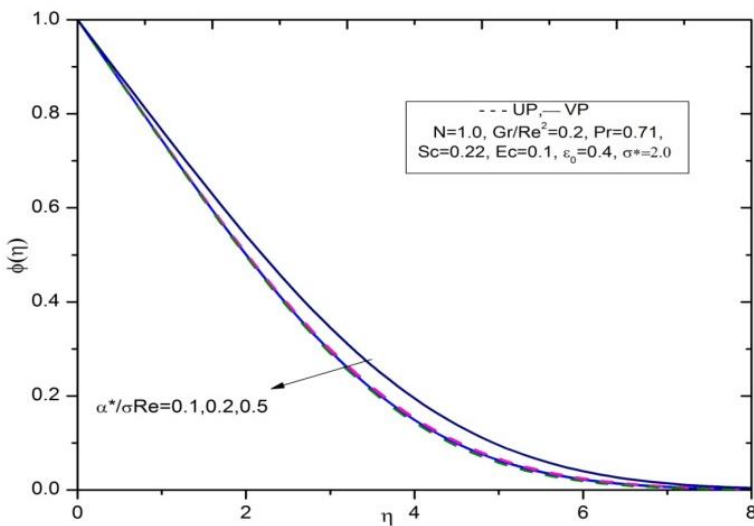


Figure 9: Concentration profiles for various values of $\alpha^*/\sigma Re$ for UP and VP cases.

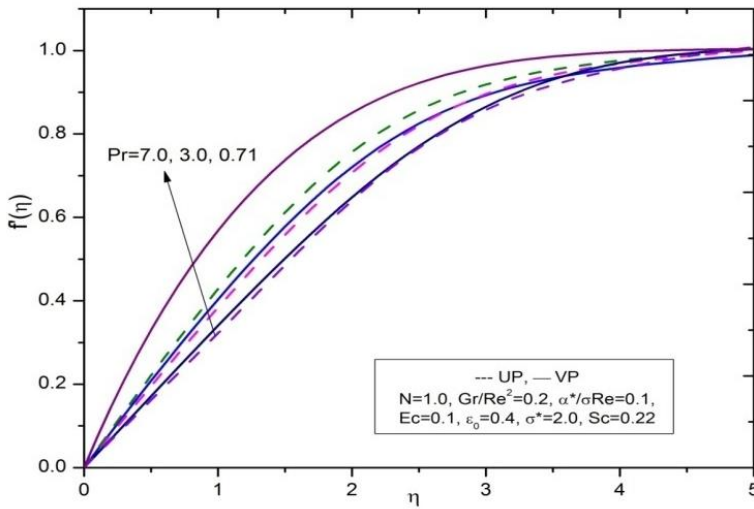


Figure 10: Velocity profiles for various values of Prandtl number for UP and VP cases.

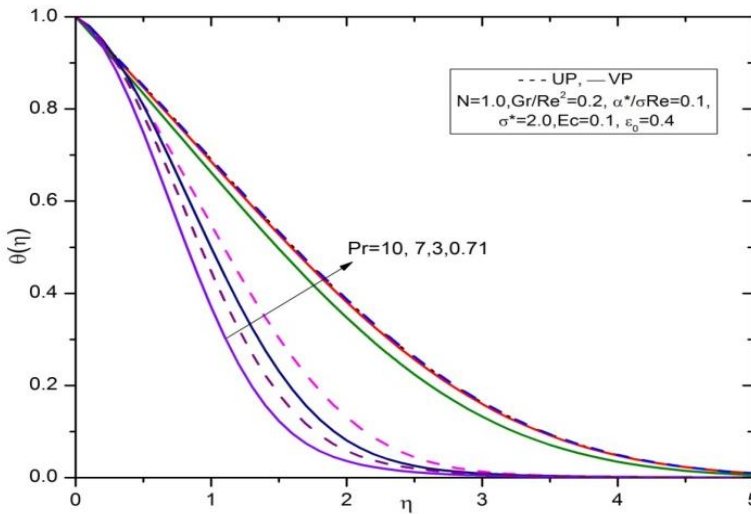


Figure 11: Temperature profiles for various values of Pr for UP and VP cases.

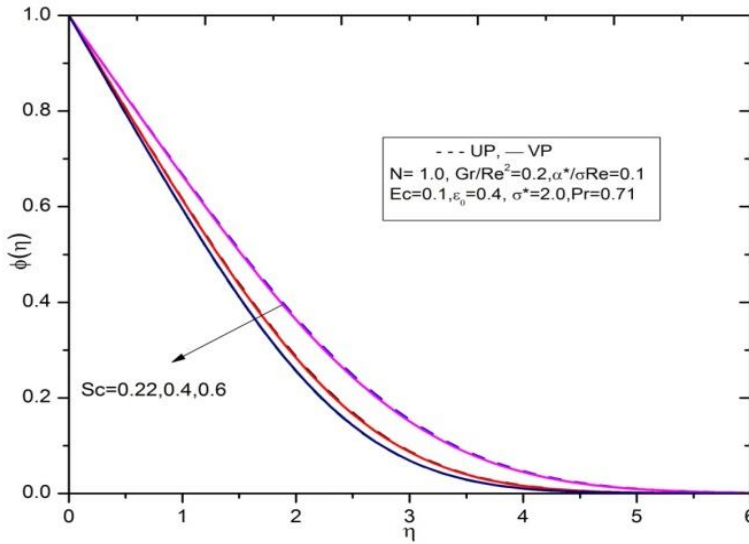


Figure 12: Concentration profiles for various values of Sc for UP and VP cases.

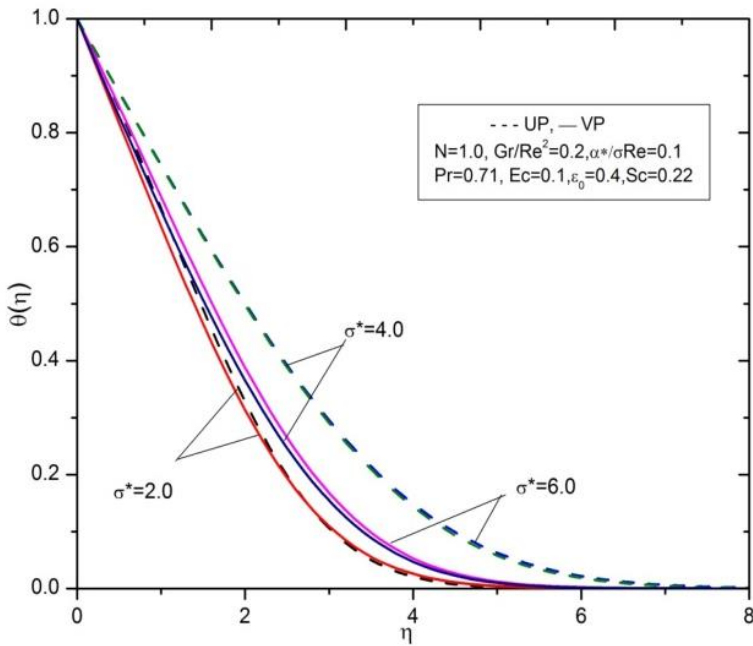


Figure 13: Temperature profiles for various values of σ^* for UP and VP cases.

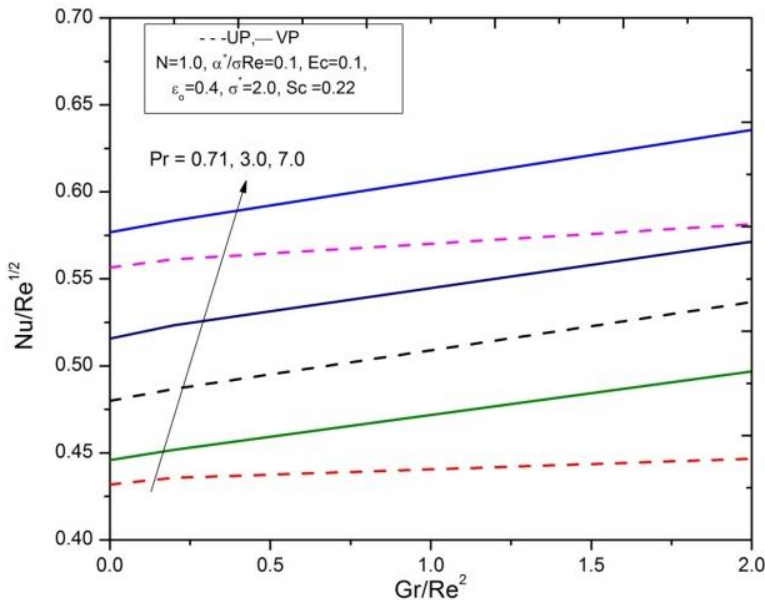


Figure 14: Variations in local Nusselt number with Gr/Re^2 for various values of Pr for UP and VP cases.

The velocity profiles for various values of mixed convection parameter Gr/Re^2 is shown in Fig. 4, it is observed that increase in value of Gr/Re^2 there is an increase in the velocity boundary layer, for higher value of Gr/Re^2 that is at $Gr/Re^2=2.0$, the velocity boundary layer increases rapidly near the plate and slowly moves down towards away from the plate. The temperature and concentration profiles for various values of Gr/Re^2 are shown in the Figs. 5 and 6. It is observed that increase in the value of the Gr/Re^2 , the profiles decreases, and for each value of Gr/Re^2 increasing, temperature profiles decreases faster compared to the concentration profiles. Here it is observed that uniform permeability dominates more than the variable permeability in velocity, temperature and concentration profiles.

Decrease in the value of local permeability parameter multiplied with the Reynolds number leads to increase in the value of $\alpha^*/\sigma Re$, the velocity profiles increases as we increase the value of $\alpha^*/\sigma Re$ as shown in the Fig. 7, this is due to Reynolds number leading to high viscous forces which has very high relative importance for giving the flow conditions and high porosity, with the moderate ratio of viscosities. Also it is observed that uniform permeability is more prominent than the variable permeability. The temperature and concentration profiles are shown in Figs. 8 and 9, it is observed that increase in the value of $\alpha^*/\sigma Re$ decreases the temperature and

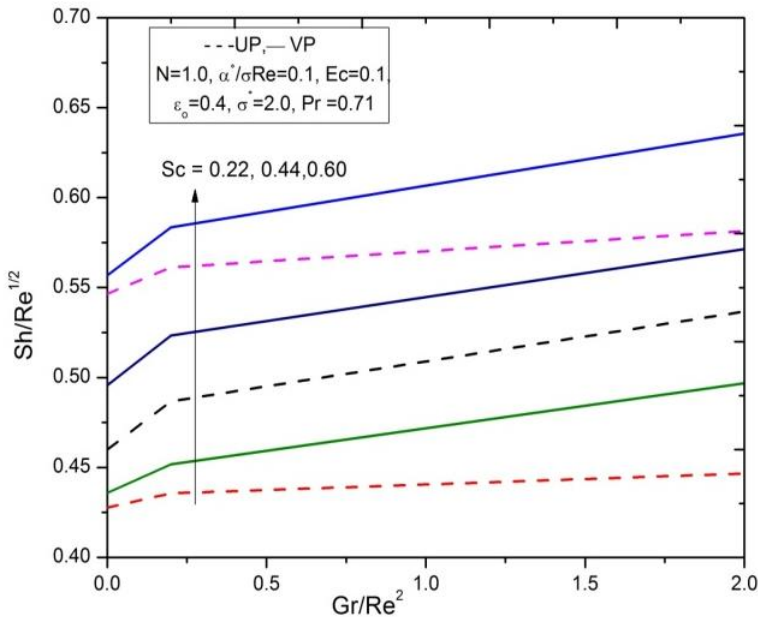


Figure 15: Variations in local Sherwood number with Gr/Re^2 for various values of Sc for UP and VP cases.

concentration profiles. It is also observed that uniform permeability and variable permeability flow behavior are same compared to any magnitude of $\alpha^*/\sigma Re$.

Increase in Prandtl number, the velocity profiles decreases which is shown in Fig. 10. It is observed that for low $Pr = 0.71$, the velocity boundary layer is high, and lowers for higher Prandtl number. Temperature distributions are shown for various values of Prandtl number in Fig. 11, it is observed that increase in Prandtl number leads to decrease in the temperature boundary layer. The temperature profile decreases rapidly for higher Prandtl number such as $Pr = 7.0$ and $Pr = 10.0$. It is also observed that the variable permeability is more prominent than the uniform permeability. Concentration distributions are shown for various values of Schmidt number in Fig. 12, it is observed that increase in the value of Schmidt number there is a decrease in the concentration profile and decays smoothly. The uniform permeability and variable permeability are showing the same behavior in the concentration boundary layer.

Variation of σ^* for temperature profiles is shown in Fig. 13. It is observed that decrease in the value of σ^* leads to decrease in the temperature profile. Both uniform permeability and variable permeability decays smoothly for all the values of

σ^* . An interesting factor can be observed here is when $\sigma^*=2.0$ both uniform permeability and variable permeability behaves same, whereas for $\sigma^*=4.0$ and $\sigma^*=6.0$ the uniform permeability slows down and not much prominent when compared to variable permeability cases.

The variations of the Nusselt number and Sherwood number as a function of Gr/Re^2 for various values of Prandtl number and Schmidt number respectively are shown in Figs. 14 and 15 for both uniform permeability and variable permeability cases. It is observed from Fig. 14 that the effect of increasing Gr/Re^2 is to decrease the Nusselt number for higher values of Prandtl number. It is also observed that from Fig. 15, the effect of increasing Gr/Re^2 is also to decrease the Sherwood number. It is clearly seen that from $Gr/Re^2=0.0$ to 0.2, there is a faster decrease and from 0.2 to 2.0 there is a moderate decrease in the Sherwood number.

5 Conclusions

In this chapter, a numerical model is developed for the study of effects of internal heat generation on mixed convection heat flow and mass transfer of an incompressible, laminar, viscous fluid past a semi infinite vertical heated plate in a saturated porous medium by considering the variable fluid properties like variable permeability, porosity and thermal conductivity. The boundary layer flow in the porous medium is governed by Lapwood-Brinkman extended Darcy model. Using the similarity variables, the governing equations are transformed into a set of highly coupled nonlinear ordinary differential equations. These equations are then solved numerically by Runge-Kutta Fehlberg method with shooting technique. The computed results in the presence of IHG are presented to illustrate the details of flow and heat and mass transfer characteristics and also their dependence on the physical parameters, the following conclusions are drawn:

1. Increase in Buoyancy ratio N is to increase the velocity distribution significantly, decrease in the temperature and concentration distribution for VP case. Initially when $N = 0$ the heat transfer is slow with the temperature boundary layer. As N increases from 0 to 1 and to 10 the heat transfer is faster in temperature distributions. Whereas, the heat transfer is slow for $N = 0$ and 1 faster for $N = 5$ and 10 in case of concentration distributions.
2. Increasing the Buoyancy force, the number Gr/Re^2 increases which lead to increase the velocity closer to the vertical heated plate. The velocity distributions are more prominent for UP when compared to VP. Increase in the parameter Gr/Re^2 enhances the temperature and concentration in the boundary layer for both UP and VP cases, and hence the fluid velocity increased. The temperature and concentration profiles for VP and UP are almost same.

3. With an increase of $\alpha^*/\sigma Re$ the velocity profile increases, decrease in the parameter $\alpha^*/\sigma Re$ enhances the temperature and concentration in the boundary layer for both cases. The profiles are less for VP compared to UP.
4. The Prandtl number shows a decreasing effect on the velocity profile as Pr increases and a rapid decreasing effect on the temperature profile as Pr increases. The boundary layer is more prominent for VP case compared to UP case. Increase of Sc enhances the concentration. For any Sc the concentration profiles for both UP and VP cases are almost same.
5. Increase in the ratio of thermal conductivity of solid to fluid σ^* decreases the temperature profiles for both UP and VP cases.
6. Increase of Pr, increases the Nusselt number and maintains the uniformity with the increase in Gr/Re^2 . This is because of the temperature difference in the Grashof number and the suitable low Reynolds number. The heat transport is more prominent for VP case when compared to UP case.
7. Increase of Sc , increases the Sherwood number. As Gr/Re^2 increases from 0.0 to 0.2 the Nusselt number increases and maintains the uniformity from 0.2 to 2.0. The mass transport is more prominent for VP case when compared to UP case.

References

- Alam, M. S.; Rahman, M. M.; Samad, M. A.** (2006): Numerical Study of the Combined Free-Forced Convection and Mass Transfer Flow Past a Vertical Porous Plate in a Porous Medium with Heat Generation and Thermal Diffusion. *Nonlinear Analysis: Modelling and Control*, vol. 11, no. 4, pp. 331-343.
- Benanati, R. F.; Brosilow, C. B.** (1962): Void fraction distribution in beds of spheres. *AIChE. J.*, vol. 8, pp. 359-361.
- Chamkha, A. J.** (2007): Heat and Mass transfer for a Non-Newtonian fluid flow along a surface embedded in a porous medium with uniform wall Heat and Mass fluxes and Heat generation or Absorption. *Intl. J. of energy*, vol.1, no. 3, pp. 97-104.
- Chandrasekhara, B. C.; Namboodiri, P. M. S.** (1985): Influence of variable permeability on combined vertical surfaces in porous medium. *International Journal of Heat Mass Transfer*, vol. 28, pp. 199-206.
- Choukairy, K.; Bennacer, R.** (2012): Numerical and Analytical Analysis of the Thermosolutal Convection in an Heterogeneous Porous Cavity. *Fluid Dyn. Mater. Process*, vol. 8, no.2, pp. 155-172.

Crepeau, J. C.; Clarksean, R. (1997): Similarity solutions of natural convection with internal heat generation. *Transactions of ASME - Journal of Heat Transfer*, vol. 119, pp. 184-185.

Ferdows, M.; Bangalee, M. Z. I.; Crepeau, J. C.; Seddeek, M. A. (2011): The effect of Variable Viscosity in double diffusion problem of MHD from a porous boundary with Internal Heat Generation. *Progress in Computational Fluid Dynamics*, vol. 11, no. 1, pp. 54-65.

Govardhan, K.; Balaswamy, B.; Kishan, N. (2012): Effects of Internal Heat Generation, Soret and Dufour on MHD Free Convection Heat and Mass Transfer in a Doubly Stratified Darcy Porous Medium with Viscous Dissipation. *Emirates Journal of Engineering Research*, vol. 17, no. 2, pp. 29-42.

Hamimid, S.; Guellal, M.; Amroune, A.; Zeraibi, N. (2012): Effect of a Porous Layer on the Flow Structure and Heat Transfer in a Square Cavity. *Fluid Dyn. Mater. Process*, vol. 8, no. 1, pp. 69-90.

Kamath, P. M.; Balaji, C.; Venkateshan, S. P. (2013): Heat transfer studies in a vertical channel filled with porous medium. *Fluid Dyn. Mater. Process*, vol. 9, no. 2, pp. 109-124.

Khalili, A.; Shivakumara, I. S. (1998): Onset of convection in a porous layer with net through-flow and internal heat generation. *Phys. Fluids*, vol. 10, pp. 315-317.

Mahmoudi, A.; Mejri, I.; Abbassi, M. A.; Omri, A. (2013): Numerical Study of Natural Convection in an Inclined Triangular Cavity for Different Thermal Boundary Conditions: Application of the Lattice Boltzmann Method. *Fluid Dyn. Mater. Process*, vol. 9, no. 4, pp. 353-388.

Mahrouche, O.; Najam, M.; El Alami, M.; Faraji, M. (2013): Mixed Convection Investigation in an Opened Partitioned Heated Cavity. *Fluid Dyn. Mater. Process*, vol. 9, no. 3, pp. 235-250.

Makinde, O. D.; Aziz, A. (2011): Mixed convection from a convectively heated vertical plate to a fluid with internal heat generation. *J. Heat Transfer*, vol. 133, no. 12, 122501 (6 pages).

Maougal, A.; Bessaïh, R. (2013): Heat Transfer and Entropy Analysis for Mixed Convection in Discretely Heated Porous Square Cavity. *Fluid Dyn. Mater. Process*, vol. 9, no. 1, pp. 35-58.

Mohamad, R. A. (2009): Double diffusive Convection radiation interaction on unsteady MHD flow over a vertical moving porous plate with heat generation and soret effect. *Applied Mathematical Sciences*, vol. 13, pp. 629-651.

Mohammadein, A. A.; El-shaer, N. A. (2004): Influence of variable permeability

on combined free and forced convection flow past a semi-infinite vertical plate in a saturated porous medium. *Heat Mass Transfer*, vol. 40, pp. 341-346.

Moufekkik, F.; Moussaoui, M. A.; Mezhab, A.; Naji, H.; Bouzidi, M. (2012): Numerical Study of Double Diffusive Convection in presence of Radiating Gas in a Square Cavity. *Fluid Dyn. Mater. Process*, vol. 8, no. 2, pp. 129-154.

Nalinakshi, N.; Dinesh, P. A.; Chandrashekhar, D. V. (2013): Numerical Study of Double Diffusive Mixed Convection with variable Fluid properties. *Intl. J. Engng. Res. & Tech.*, vol. 2, Issue 9, pp. 131-139.

Olanrewaju, P. O.; Arulogun, O. T.; Adebimpe, K. (2012): Internal heat generation effect on thermal boundary layer with a convective surface boundary condition. *American Journal of Fluid Dynamics*, vol. 2, no. 1, pp. 1-4 .

Pal, D.; Shivakumara, I. S. (2006): Mixed Convection heat transfer from a vertical heated plate embedded in a sparsely packed porous medium. *Int. J. Appl. Mech. Eng.*, vol. 11, pp. 929-939.

Pal, D. (2010): Magneto hydrodynamic non-Darcy mixed convection heat transfer from a vertical heated plate embedded in a porous medium with variable porosity. *Commun. Nonlinear Sci. Numer. Simulat.*, vol. 15, pp. 3974-3987.

Patil, P. M.; Kulkarni, P. S. (2008): Effects of Chemical reaction on free convective flow of a Polar fluid through a porous medium in the presence of internal heat generation. *Int. J. therm. Sci.*, vol. 4, pp. 1043-1054.

Schwartz, C. E.; Smith, J. M. (1953): Flow distribution in packed beds. *Ind. Eng. Chem.*, vol. 45, pp. 1209-1218.

Seddeek, M. A. (2005): Finite Element Method for the effects of chemical Reaction, Variable viscosity, thermophoresis and Heat Generation / Absorption on a Boundary layer Hydro Magnetic flow with heat and Mass transfer over a Heat surface. *Acta Mechanica*, vol. 177, pp. 1 -18.

Selimos, B.; Poulikakos, D. (1985): On double diffusion in a Brinkman heat generating porous layer. *Int. Comm. Heat Mass Transfer*, vol. 12, pp. 149-158.

Vajravelu, K. (1980): Effects of variable properties and internal heat generation on natural convection at a heated vertical plate in air. *Numerical Heat Transfer*, vol. 3, no. 3, pp. 345-356.

Vajravelu, K.; Hadjinicolaou, A. (1993): Heat Transfer in a viscous fluid over a stretching sheet with viscous dissipation and internal heat generation. *Int. Commun. Heat Mass Transfer*, vol. 20, pp. 417-430.